# Investigation of Cell Growth and Chlorophyll *a* Content of the Coccolithophorid Alga *Emiliania huxleyi* by Using Simple Bench-Top Flow Cytometry

Ioanna Hariskos*, Tobias Rubner and Clemens Posten

*Institute of Process Engineering in Life Sciences, Karlsruhe Institute of Technology, Germany*

## Abstract

The coccolithophorid alga *Emiliania huxleyi* produces micro-structured calcite particles, which are called coccoliths. Due to their unique and sophisticated structure, coccoliths are highly promising for different industrial applications, such as paper manufacturing, color and lacquer preparation. The mass production of coccoliths requires the evaluation of optimum cultivation conditions. This study investigates the impact of varying irradiance (10-1500 µmol m$^{-2}$ s$^{-1}$) on growth and chlorophyll *a* content of two calcifying strains CCMP371 and RCC1216 as well as on the non-calcifying strain RCC1217 (haploid form of RCC1217). The light kinetics contradicts the popular opinion, that *E. huxleyi* is an extraordinarily light tolerating alga in general. Photoinhibition was already observed at irradiance >500 µmol m$^{-2}$ s$^{-1}$ in the case of the calcifying strains. Furthermore, light requirements to grow at maximum growth rate, as well as thresholds towards photoinhibition were considerably different between calcifying and non-calcifying strains. The haplont required significantly higher irradiance to reach maximum µ$_{spec}$ (>200 µmol m$^{-2}$ s$^{-1}$), while being much more tolerant to towards photoinhibition, which occurred not until 800 µmol m$^{-2}$ s$^{-1}$. Furthermore, a novel method was proposed to allow for the estimation of chlorophyll *a* content from flow cytometry data. By comprising an Advanced Fluorescence Ratio (AFLR), which considers culture heterogeneity, this method enables for simple chlorophyll *a* estimation also in older cultures of calcifying *Emiliania huxleyi*, which tend to build agglomerates.

**Keywords:** Microalgae characterization; Chlorophyll; Autofluorescence; Flow cytometry; Photosynthetic pigments

**Abbreviations:** AFLR: Advanced Fluorescence Ratio; CV$_{\%}$: Coefficient of Variation; ESAW: Enriched Seawater Artificial Water; FSC: Forward Scatter; FLR: Fluorescence Ratio; MFI: Median Fluorescence Intensity; SSC: Sideward Scatter

## Introduction

Microalgae have been shown to be industrially important microorganisms and offer a large product portfolio which include biofuels, pigments, polyunsaturated fatty acids, and vitamins [1,2]. Apart from these organic products, some microalgae are able to build inorganic particles by intracellular calcification [3-5]. The coccolithophorid alga *Emiliania huxleyi* produces high numbers of external micro-structured calcite platelets, called coccoliths, which coat their entire cell surface. Coccoliths are of unique and highly sophisticated three-dimensional structure, which cannot be artificially imitated. They consist of calcite crystals with uniform crystal lattices and have a narrow size distribution [6]. Therefore, coccoliths are a potential resource for several novel applications, such as paper manufacturing, color- and lacquer preparation, and even laser optics [7].

The production of coccoliths within the coccolithophores requires the development of a highly regulated bioprocess. Both growth and calcification are light-dependent processes [8-10]. Optimum mostly refers to a certain irradiance, which enables the cells to grow with maximum rate, also called photosaturation. While irradiance below light saturation causes growth limitation, excessive illumination leads to a reduction in PSII activity photoinhibition. That means the inhibition of photosynthesis by energetic oversaturation of the photosynthetic apparatus. It is therefore beneficial to know the light kinetics of the organism of choice and therefore the range of photosaturation. In the case of *E. huxleyi*, it is often claimed, that this alga is extremely light tolerable and experiences no detectable photoinhibition, even at full daylight [11]. However, attempts to grow two different calcifying

strains (RCC1216 and CCMP371) under comparable conditions resulted in limited success (unpublished results). It is for this reason that light-tolerance does not necessarily need to be equally pronounced in every strain of *E. huxleyi*. It is therefore decisive to assess optimum irradiance for every single production strain.

In most cases, chlorophyll *a* content is used as a normalization factor for a variety of metabolic parameters. Examples are the photosynthesis rate, metabolically active biomass, and the productivity of terrestrial or aquatic ecosystems [12]. However, classic protocols for optical chlorophyll *a* quantification are not always suitable in daily sampling routine. Direct estimation of the chlorophyll *a* content from photometric absorption data is not feasible. This technique fails to reflect all chlorophyll *a* in the cell, especially when cells aggregate. For this reason, chlorophyll *a* is almost always extracted first and subsequently analyzed by photometry or chromatography. This requires at least a certain amount of biomass for one single measurement, which often leads to large sample volumes. Secondly, toxic solvents plus time-consuming analytical techniques make conventional extraction methods rather user-unfriendly. Even though optical chlorophyll *a* analysis is quite precise, measurements only

**\*Corresponding author:** Ioanna Hariskos, Karlsruhe Institute of Technology, Institute of Process Engineering in Life Sciences, Section III Bioprocess Engineering, Building 30.44, Fritz-Haber-Weg 2, D- 76131 Karlsruhe, Germany, Tel: +49-721-608- 452-04; E-mail: ioanna.hariskos@kit.edu

reflect averaged values over living and dead cells, giving no information about heterogeneity within a culture. A more comfortable method for chlorophyll *a* quantification at regular intervals would therefore be a rapid cell-by-cell analysis technique like flow cytometry. In the case of microalgae cultivation, it is usually used for discrimination and quantification of different photoautotrophic species in phytoplankton assemblages [13-15]. This is comparably simple because phototrophic cells can be distinguished easily from any background particles by their red autofluorescence which almost exclusively (90-95%) derives from the red fluorescence of chlorophyll *a* (emission >610 nm) [16,17]. In contrast to natural, highly diluted phytoplankton communities, dense microalgal cultures are necessary for production purposes. Those cultures show high deviations in cell-specific chlorophyll *a* concentrations over the duration of cultivation. This is particularly true, if the increasing cell number leads to environmental stress like mutual shading or substrate limitation [18,19]. Nevertheless, it would be very comfortable to calculate the actual chlorophyll *a* content from cytometric fluorescence data.

The objective of this study is to asses light kinetics and chlorophyll *a* content by using a simple bench-top flow cytometer. Therefore, a novel method for chlorophyll *a* quantification is presented, which simplifies chlorophyll *a* quantification in daily lab routine. This information might support the development of future cultivation strategies in production-scale.

## Material and Methods

### Culture conditions

Axenic flask cultures of two different diploid and calcifying strains of *E. huxleyi* (CCMP371, RCC1216) were used in the experiment (Figure 1). These two strains were selected to evaluate differences between "high" calcified (RCC1216) and "lower" calcified coccoliths (CCMP371). Additionally, the non-calcifying strain RCC1217 was investigated, which represents the haploid life form of the strain RCC1216. All strains possess similar maximum specific growth rates of approximately 1 $d^{-1}$ and are currently subject to process development for coccolith production.

For determination of the specific light kinetics, all strains were grown in 250 ml sterile ESAW medium (according to Berges et al. [20]) in 500 ml Erlenmeyer flasks at 21°C under continuous illumination with warm-white LEDs (Nichia NS67L183BT) at different irradiance (10, 20, 50, 100, 300, 400, 500, 800, 1500 $\mu mol\ m^{-2}\ s^{-1}$). Cultures were

agitated by an orbital shaker at 100 rpm to prevent cell settling and to ensure homogeneous illumination. The non-calcifying strain RCC1217, which is the haploid and non-calcifying variant of RCC1216, was not shaken, but suspended daily by gently shaking the flasks before every sampling. This was necessary as this strain has been shown to be sensitive to continuous mixing in other experiments (unpublished results). Cultures grown at irradiance below 100 $\mu mol\ m^{-2}\ s^{-1}$ were covered with lightproof boxes in order to shield the cultures from any interfering background light. Pre-cultures were acclimatized to illumination and cultured for at least 10 days until growth had reached the late exponential phase (< $10^6\ ml^{-1}$) before sub-culturing into the main culture. The starting cell concentration was $10^4\ ml^{-1}$ in each cultivation. Sampling was carried out daily for a total of 12 days. To validate cell conditions and axenicity, culture broth was regularly checked for contaminants. Specific growth rates were determined by exponential regression over at least 4 data points within the culture log-phase ($R^2$>0.98).

### Flow cytometry: Determination of growth and autofluorescence

For determination of growth and autofluorescence, the bench-top flow cytometer Guava EasyCyte 6-2L (Merck, Millipore) and the matching software Incyte 2.7 were used. The cytometer was provided with two collinear modulated lasers, a blue laser (488 nm → filter bandpass 690/50=RED) and a red laser (642 nm → filter bandpass 661/19=RED2). It was necessary to trigger maximum fluorescence $F_{max}$. This is the case when the photosynthetic reaction centers are closed, which means that they are saturated with electrons. The fluorescent signal then reflects the quantities of fluorescing pigment. Therefore, the cells must be illuminated with a high dose of photons for a certain amount of time. A pulse of 2000-6000 $\mu mol\ m^{-2}\ s^{-1}$ for ≤1 s is sufficient to close all reaction centers of the photosynthetic apparatus and to achieve $F_{max}$ [21]. Laser irradiances were measured directly (Li-Cor Light Meter LI-250A) and determined to be 5500 $\mu mol\ m^{-2}\ s^{-1}$ (blue laser) and 6100 $\mu mol\ m^{-2}\ s^{-1}$ (red laser), respectively. The volume flow rate was set to 0.59 $\mu l\ s^{-1}$. To create a reference point for chlorophyll *a* autofluorescence measurement, a suitable internal standard, for example commercially available fluorescent particles was employed. This is necessary in order to avoid systematical errors (temperature and laser power fluctuations) and as well to control the quality of device performance [22]. Therefore, 195 $\mu l$ cell suspension were mixed with 5 $\mu l$ bead solution (Guava EasyCheck beads). If cell concentration exceeded $5 \times 10^5\ ml^{-1}$, samples were diluted with particle-free ESAW.
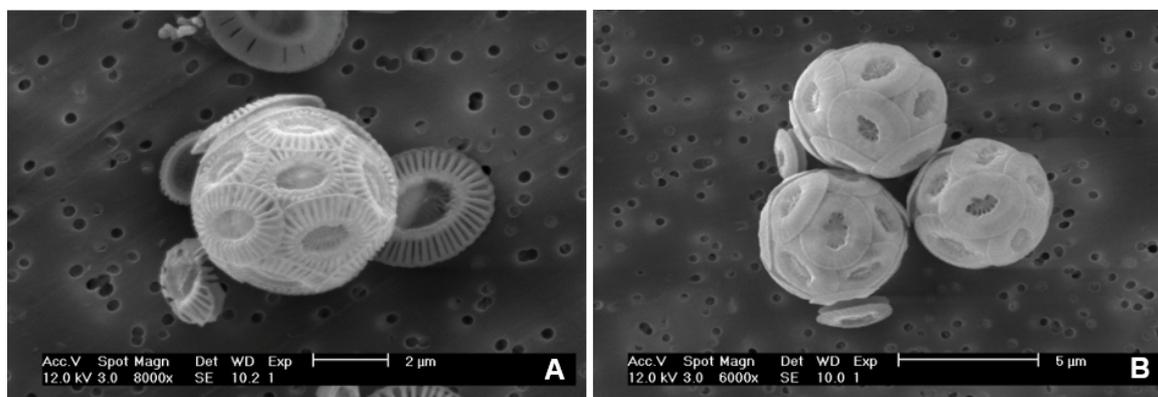


**Figure 1:** Environmental Scanning Electron Microscopy (ESEM) pictures of two calcifying strains of *Emiliania huxleyi*. A) Low calcifying strain *E. huxleyi* CCMP371 with apparent grooves between the distal shield elements. B) *E. huxleyi* RCC1216 with gapless crystal shield elements.

Cell concentration was determined by gating over the RED/RED2 fluorescence (both 5 decade acquisition). For the estimation of autofluorescence, the median fluorescence intensity (MFI) of the RED and RED2 fluorescence of the cell population and beads was monitored and used for calculation. Prior to fluorescence measurements, the linear range of the photomultiplier tube was checked with BD Calibrite Blank Beads. The coefficients of variation ($CV_{\%}$) at different gain settings for RED and RED2 were compared.

### Photometric chlorophyll determination

The method used for direct chlorophyll extraction was based on different established protocols [12,23]. A culture suspension containing $2 \times 10^7$ cells (*E. huxleyi* CCMP371, RCC1216) and $8 \times 10^7$ (RCC1217), respectively, was centrifuged in 50 ml or 15 ml falcon tubes (10 min, 4°C, 11,000 and 28,000 g, respectively) depending on the sample size. The pellet was washed with 1 ml deionized water. After a second centrifugation step (10 min, 4°C, $11,000/28,000 \times g$), 1000 µl of extraction solvent (90% acetone saturated with $CaCO_3$) was added to the pellet and suspended. Incubation occurred for 30 min at room temperature. The suspension was subsequently centrifuged (10 min, 4°C, $11,000/28,000 \times g$). To harvest the raw extract, 950 µl of supernatant was carefully transferred to a fresh 1.5 ml test tube. Testing revealed that raw extracts can be stored at -20°C for two weeks at the maximum. Before measurement, the raw extract was centrifuged at high gravitation (5 min, 4°C, $31,000 \times g$) and 800 µl of final extract was transferred to acetone-resistant cuvettes (10 mm). Measurement was carried out in a spectrophotometer (PerkinElmer Lambda 35). Since extracts had to be particle-free for measurement, absorption of <0.005 AU at 750 nm was mandatory. For all measurements, the extraction solution (see above) was used as a blank. Chlorophyll *a* concentration of the extracts was determined by absorption at λ=630 nm and λ=664 nm using the following equations [12]:

$$c\left(\text{Chl }a\right)\left[\frac{\mu g}{mL}\right] \approx E_{\lambda 1,a} \times A_{\lambda 1} + E_{\lambda 2,a} \times A_{\lambda 2}$$

$$630 \text{ nm}: E_{\lambda 1,a}\left[\frac{\mu g \text{ cm}}{mL \text{ AU}}\right] = -0.4504$$

$$664 \text{ nm}: E_{\lambda 2,a}\left[\frac{\mu g \text{ cm}}{mL \text{ AU}}\right] = 11.4902$$

The calculation is valid for a light path of d=1 cm.

### Results

Cultivation at varying irradiance exhibited a noticeable difference in the shape of light kinetics in the three tested strains (Figure 2). Both calcifying strains (CCMP371, RCC1216) were light-saturated already at 100 µmol m$^{-2}$ s$^{-1}$ (CCMP 371 $\mu_{max} \approx 1$ d$^{-1}$, RCC 1216 $\approx 0.9$ d$^{-1}$). A higher photon flux density near 300 µmol m$^{-2}$ s$^{-1}$ was necessary for the haplont to reach maximum growth rate ($\mu_{max} \approx 1.1$ d$^{-1}$). The differences in light kinetics were even more obvious regarding the range of light saturation. The haplont tolerated much higher irradiance up to 800 µmol m$^{-2}$ s$^{-1}$ before inhibition was observed. In contrast, light-saturation ranged only between 100-500 µmol m$^{-2}$ s$^{-1}$ in the calcifying strains. Interestingly, the slope in $\mu_{spec}$ over increasing irradiance was rather similar up to 100 µmol m$^{-2}$ s$^{-1}$ in all tested strains, which reflects similarities in photosynthetic efficiencies. Microscopy revealed that the cultured cells differed in size and shape. This was particularly the case at a later stage of the cultivation (stationary phase) when the morphological properties of the culture changed dramatically. This was observed on

the single cell level as well as on the entire population level. As depicted in Figure 3A, stationary-phase culture broths of the calcifying strain RCC1216 were highly heterogeneous, containing calcifying and naked cells as well as aggregates of cells and coccoliths. This was also shown by the scatter and fluorescence plots of these cultures: Calcifying cells which represented the main fraction of the population were mapped as a central dense cluster of points in the scatter plot (FSC/SSC plot). Naked cells diffused the light much less and therefore produced less side scatter, while complex particles like agglomerates were reflected by much higher scatter on the SSC axis. When looking at the fluorescence histograms obtained from flow cytometry, fluorescence distribution appears to follow a log-normal distribution. A log-normal distribution of cell volume in a cell population was originally assumed in blood cell research, can be transferred to many biological systems, and will also be assumed here [24]. This type of distribution directly reflects the three-dimensional character of the cells. Photosynthetic organisms possess a very high red autofluorescence due to the fluorescence of chlorophyll *a*, which is located inside the chloroplasts. If a cell has a diameter that is twice the diameter of another cell, its volume is about 8-times bigger than that of the other cell. Thus, the larger organelles are located inside this cell. This also includes chlorophyll *a* inside the thylakoid membranes of the chloroplasts, which also increases with a factor of 8 in an ideal model. Since the chlorophyll *a* content varies from cell to cell with r³, red fluorescence data are also distributed log-normally. Of course, the inner filter effect has to be neglected to some extent, since every chlorophyll is supposed to be excited by the laser beam and every emitted photon reaches the detector. As shown in the figure, the grade of morphological heterogeneity was observable both by light
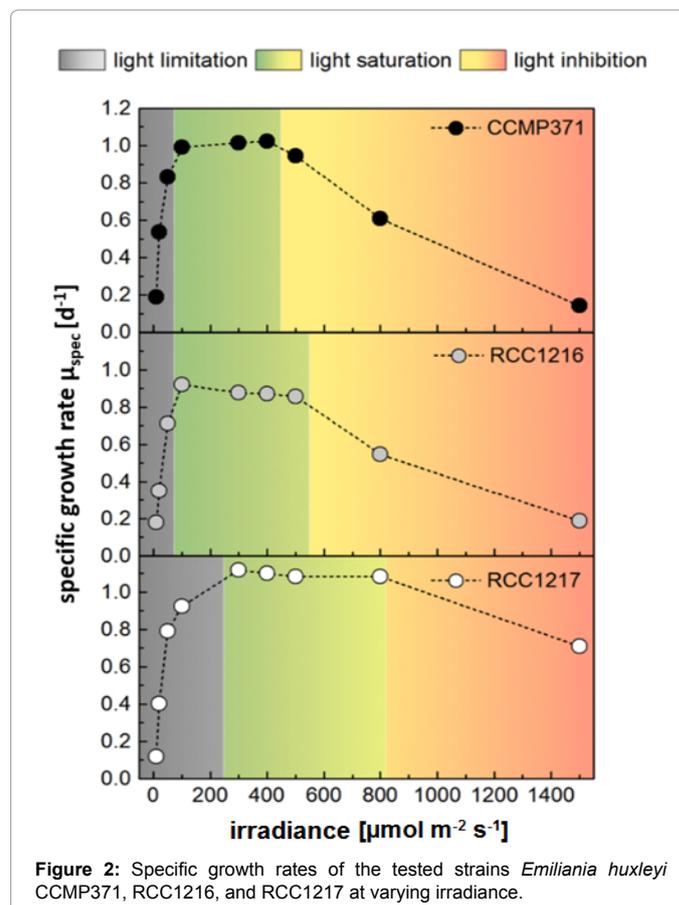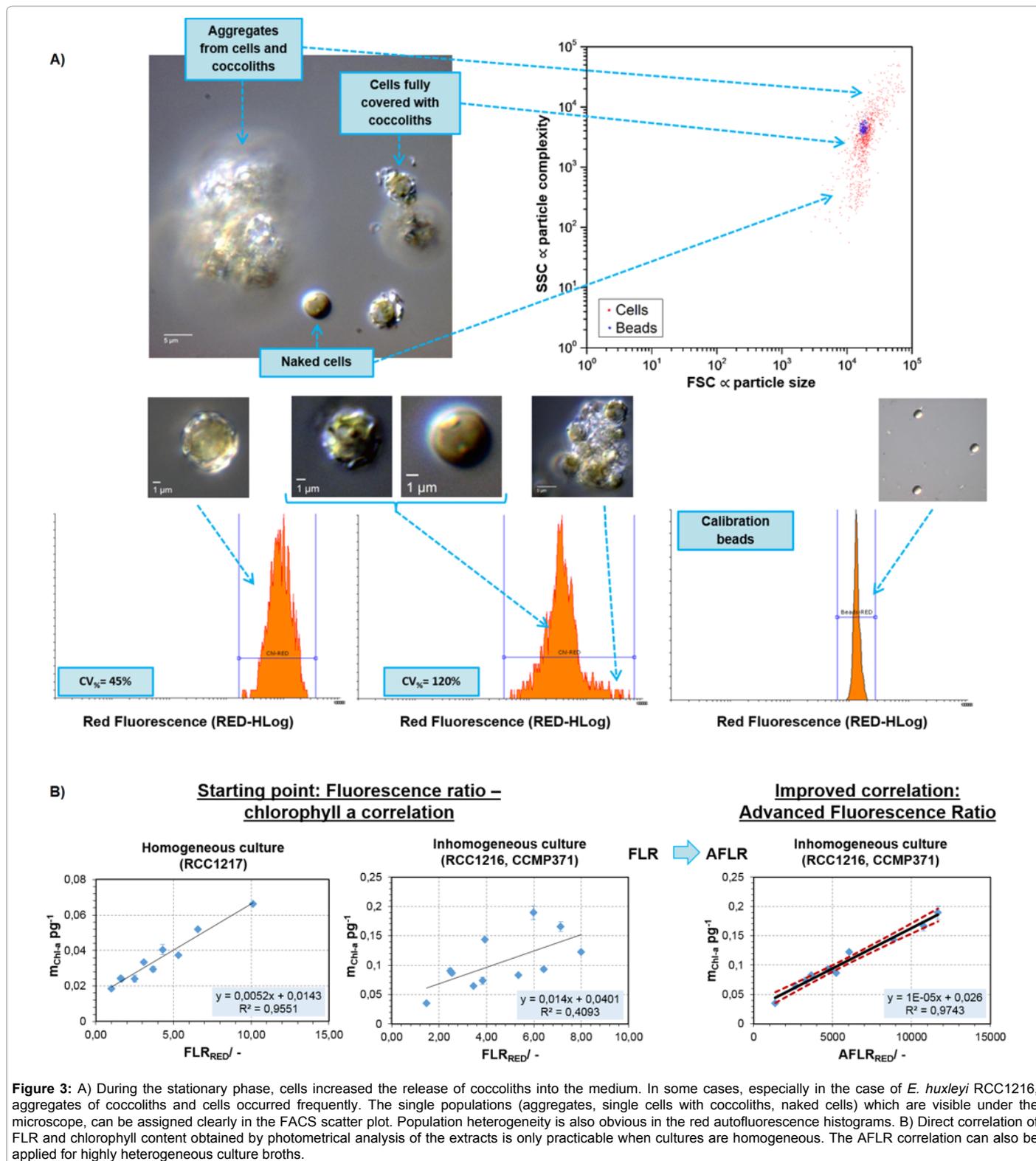


**Figure 2:** Specific growth rates of the tested strains *Emiliania huxleyi* CCMP371, RCC1216, and RCC1217 at varying irradiance.

**Figure 3:** A) During the stationary phase, cells increased the release of coccoliths into the medium. In some cases, especially in the case of *E. huxleyi* RCC1216, aggregates of coccoliths and cells occurred frequently. The single populations (aggregates, single cells with coccoliths, naked cells) which are visible under the microscope, can be assigned clearly in the FACS scatter plot. Population heterogeneity is also obvious in the red autofluorescence histograms. B) Direct correlation of FLR and chlorophyll content obtained by photometrical analysis of the extracts is only practicable when cultures are homogeneous. The AFLR correlation can also be applied for highly heterogeneous culture broths.

microscopy and flow cytometry and logically influenced the shape of the red autofluorescence histogram. Young cultures which contained only calcifying cells in exponential-phase growth as well as rather homogeneous cultures of RCC1217 showed a comparatively narrow fluorescence distribution, which can be easily identified as a log-normal distribution because the values are normally distributed around a geometric mean (=median in a log-normal distribution) when plotted logarithmically. The ideal shape changes with increasing heterogeneity. Especially aggregates which can be assigned to the right shoulder of the peak cause a severe widening of the peak width. Measurements of

a homogeneous culture from the exponential growth phase showed much lower $CV_\%$ between 20-40%. Older cultures exhibited much higher $CV_\%$ in red fluorescence with >100%. In cultures of CCMP371 and RCC1217 peak broadening was not observed in the process of cultivation and $CV_\%$ remained rather constant. A direct correlation of FLR and the photometrically determined chlorophyll *a* data points revealed an acceptable correlation in the case of RCC1217 only, where cells were highly homogeneous in shape and size (Figure 3B). In all other cases, correlation was very weak ($R^2 \sim 30\%$) and, hence, not practicable. For this reason, direct plotting was inappropriate to estimate the intracellular chlorophyll content directly from the fluorescence intensity measured by flow cytometry. To improve the correlation, several considerations had to be made. It was obvious that population heterogeneity had to be incorporated in a practical correlation of FLR and chlorophyll concentration. As previously stated, autofluorescence data measured by flow cytometry are distributed log-normally due to the biological variability. For log-normal distributions, it is favorable to use median instead of the arithmetic mean for calculation.

For this reason, the MFI of the cells and the MFI of the beads were used for further calculations. To linearize the distance between the peaks of cells and beads, the respective MFIs were logarithmized. These two values were related to each other to give a reference point (beads) for chlorophyll *a* detection.

A second key issue was to additionally include the widening of the peak with morphological heterogeneity. For this, the best option was to use the area of the peak. Since this information was not given by every flow cytometry analysis software, the coefficient of variation ($CV_\%$) was related to the MFI of the autofluorescence. This corresponds to a simplification of the fluorescence peak area, but is easier to calculate with the available data. Applying these considerations, the following term for an advanced fluorescence ratio (AFLR) was used:

$$AFLR = \frac{\log_{10}(\mathrm{MFI_{Chl}})}{\log_{10}(\mathrm{MFI_{Beads}})} \times \left[ \frac{CV_{\%Chl}}{100\%} MFI_{Chl} \right]$$

When using the AFLR instead of the FLR for correlation, the coefficient of determination was improved to $R^2=97.2\%$ in the case of RCC1216. This demonstrates very clearly that morphological heterogeneity plays a crucial role in the correlation of fluorescence

and should not be neglected. In addition, a confidence band was calculated for the regression line by using the variance/covariance matrix [25]. For further statistic coverage, it is appropriate to presume a student t-distribution instead of a normal distribution. The student t-distribution gives additional weighting to the number of samples, which also enhances regression confidence.

Figure 3B also shows the correlation of AFLR with the photometrically determined chlorophyll *a* concentration within the 95% confidence interval. Inside the red dotted line, 95% of all possible values of the population are located. For statistical reasons, the confidence is highest in the middle of the regression line. This method was tested for all strains and the corresponding equations for correlation were determined (Table 1). The general equation can be expressed as follows:

$$mChla \approx a \times AFLR_{RED} + b$$

The AFLR-correlation coefficient was higher for the strains CCMP371 and RCC1216 than for the FLR correlation (Table 1). This was not valid for the strain RCC1217, which showed a slightly better correlation using the FLR (95.51% compared to 93.73%).

As shown in Figure 4, measured and calculated chlorophyll data were in good agreement. It is obvious that all three strains significantly differed in their chlorophyll content during cultivation. Chlorophyll *a* concentrations in the haploid strain RCC1217 remained rather constant, while the calcifying strains changed noticeably, especially upon entry into the stationary phase. The strain CCMP371 reduced the chlorophyll *a* content per cell to approximately 50% of the maximum concentration, while RCC1216 first increased (+150%) in concentration in the early stationary phase and then decreased it again at the end (day 11/12) of the cultivation.

However, the chlorophyll content substantially differed between strains and cultivation conditions, even when all samples were taken from exponential phase (Figure 5). Cells expressed generally more chlorophyll *a* at lower irradiance, with the chlorophyll content being also lower under light-limiting conditions. Both calcifying strains contained similar intracellular concentrations on the average, except under light-limiting conditions, where the strain CCMP371 expressed consistently less chlorophyll *a*. The haploid strain showed similar
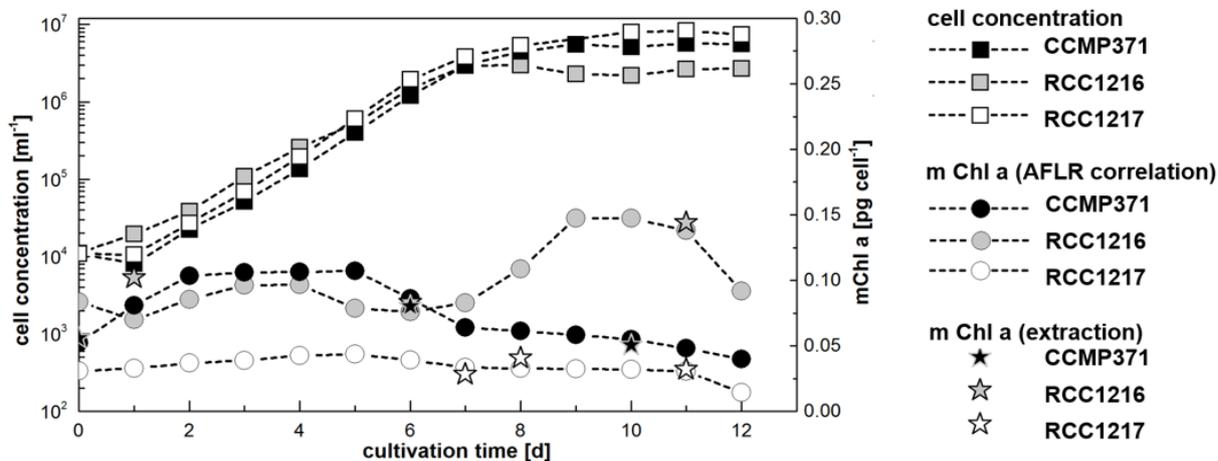


**Figure 4:** Changes in cell concentration and chlorophyll content during cultivation. All strains were illuminated with 300 µmol m$^{-2}$ s$^{-1}$ (light-saturation). Measured (circles) and calculated (X) chlorophyll concentration values from AFRL correlation.

| Strain | Slope a [$pg_{Chla}$ $cell^{-1}$] | y-intercept b [$pg_{Chla}$ $cell^{-1}$] | Coefficient of determination $r^2$ [%] |
|---|---|---|---|
| CCMP371 | $1.97411 \times 10^{-5}$ | $1.60053 \times 10^{-2}$ | 96.81 |
| RCC1216 | $1.36618 \times 10^{-5}$ | $2.60306 \times 10^{-2}$ | 97.43 |
| RCC1217 | $5.20385 \times 10^{-3}$ | $1.42561 \times 10^{-2}$ | 95.51 (FLR correlation) |
| RCC1217 | $1.24632 \times 10^{-5}$ | $9.34275 \times 10^{-3}$ | 93.73 (AFLR correlation) |

**Table 1:** Parameters for the calculation of intracellular chlorophyll concentration in the tested strains by AFLR$_{RED.}$
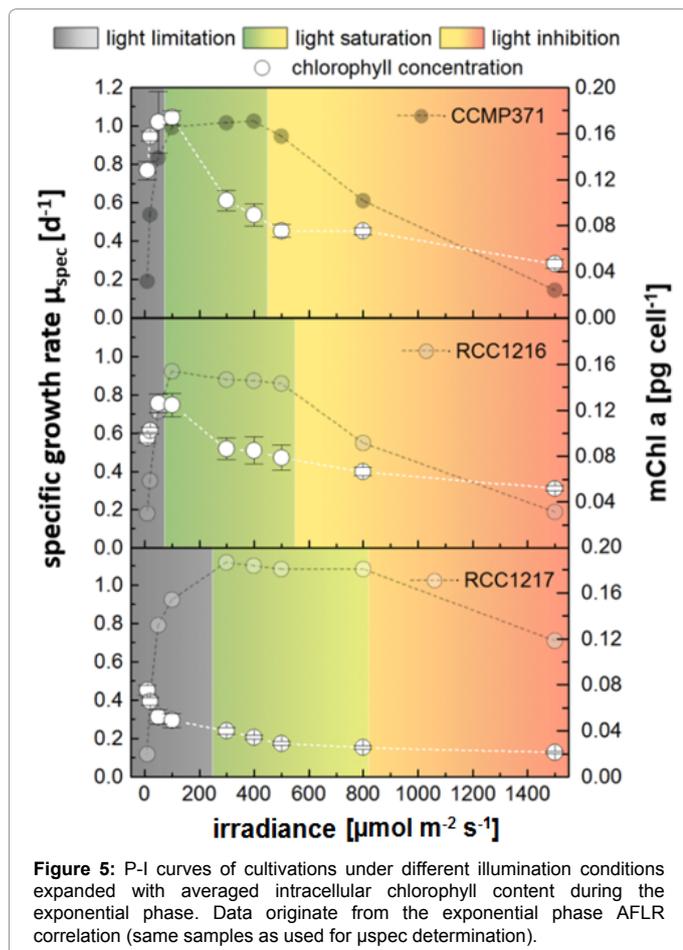


**Figure 5:** P-I curves of cultivations under different illumination conditions expanded with averaged intracellular chlorophyll content during the exponential phase. Data originate from the exponential phase AFLR correlation (same samples as used for μspec determination).

behavior under varying irradiance, but contained approximately 50% less chlorophyll in any case.

## Discussion

All tested strains were subject to severe photoinhibition at irradiance above 800 μmol $m^{-2}$ $s^{-1}$, with the haploid, non-calcifying strain RCC1217 being tolerant (growing with $μ_{max}$) to twice the irradiance compared to the diploid life-cycle stage RCC1216. This is inconsistent with previous studies, in which calcifying *E. huxleyi* showed a much higher photo tolerance, with photoinhibition beginning not until 1000-1400 μmol $m^{-2}$ $s^{-1}$ (strains BOF92 and CCCMP1571) [26,27]. In contrast to this, photoinhibition was found to occur already at a much lower irradiance of 500 μmol $m^{-2}$ $s^{-1}$ in a non-calcifying strain [27]. Even though it was earlier assumed that coccoliths may have a photo-protective function and their production increases with irradiance [8-10,28], our results confirm the current opinion, that coccoliths do not protect from excessive light influx [27]. It is obvious that results of single studies cannot be generalized, especially when different strains and illumination profiles, such as day/night cycles, are implemented. Additionally, techniques for irradiance measurement are not uniform and often incomprehensible in different labs. However, the assumption, that *E. huxleyi* is an extraordinarily light tolerating alga in general, should be reconsidered.

All tested strains showed a steady decrease of the chlorophyll *a* content with increasing irradiance, as is does in all algae, since it is a normal part of photo acclimation [29]. Interestingly, the haploid strain RCC1217 had only half of the chlorophyll *a* content per cell, while needing approximately twice the amount of photons to grow with $μ_{max}$, which is consistent with the observed higher photo tolerance. On the genetic level, it is already known that cells in both life-cycle stages express certain genes to different extents [30,31]. The haploid strain is genetically much more efficiently organized, which suggests the lower energy requirement [30] and may result in a higher metabolic capacity for the protective systems. This may make the haploid stage of *E. huxleyi* a more robust, persistent vegetative spore [8].

However, the results indicate that both calcifying strains should be cultivated in the range of 100-500 μmol $m^{-2}$ $s^{-1}$ to support maximum growth rate. This has consequences for the design of a suitable cultivation environment, which should protect from excessive irradiance, especially in outdoor concepts, when sunlight is used. At the same time, the reactor should prove enough light to support photosaturation, even at high cell densities where cells and coccoliths shade each other. Suitable approaches may be light dilution reactors with low layer thickness, where the incident sunlight is spread over a larger reactor surface area [32].

The chlorophyll *a* values calculated from correlation were in good agreement with the values measured by photometrical detection. The developed method meets the requirements for a successful determination of the chlorophyll *a* content via red autofluorescence data. The irradiance of both lasers emitted at least around 5500 μmol photons $m^{-2}$ $s^{-1}$, which resulted in the emission of maximum chlorophyll fluorescence $F_{max}$. This was also confirmed in another experiment, in which cells were dark adapted for 10 minutes before passing through the flow cytometer, but showed no difference in fluorescence emission (data not shown). In a study with spinach it was shown that it is generally possible to excite chlorophyll *a* to maximum fluorescence with flow cytometer-integrated laser beams [33]. Other studies predict that the measured fluorescence signal is located between $F_0$ and $F_{max}$ [34]. This might be the case, if laser power is not sufficient to close all reaction centers of the photosynthetic apparatus. The suitability of this protocol must therefore be evaluated for the available flow cytometer. Sosik et al. already showed that there must not necessarily be coherence between measured autofluorescence and intracellular chlorophyll content [35]. However, their calculations were based on the arithmetic mean instead of the median. Since fluorescence data were log-normally distributed, fluorescence was weighted differently than in this study. Additionally, these authors also examined the calcifying algae *Hymenomonas carterae* and the diatom *Thalassiosira weissflogii* in their studies. Data presented in this study has shown that calcification supports morphological heterogeneity during cultivation. When comparing their study with the data presented here, it can be suggested that AFLR led to a significant improvement of the correlation between their measured fluorescence and the chlorophyll *a* content.

It is also noticeable that their FLR correlation and their obtained fluorometry data were quite similar. On a technical level, however, flow cytometry offers a decisive advantage over fluorometry: Fluorometry

measures the fluorescence of the entire cell suspension only. A flow cytometer detects the fluorescence of single cells. From this, fluorescence distributions can be derived. This enormously enlarges the scope of data information and the variation coefficient supplies direct information on the culture quality.

As shown in Figure 3, morphological heterogeneity increased during the process time. This depended on the strain type as well as on the cell cycle (haploid or diploid). During the stationary phase, production of coccolith-associated extracellular polysaccharides increases [27], which supports agglomeration [36]. In our experiments, agglomerates showed a particularly high autofluorescence. This may be explained by the functioning of the flow cytometer, which counts aggregates as single particles, leading to a higher fluorescence signal. It is also possible that cells which are located inside the aggregates express more chlorophyll to compensate the loss of photons due to shading caused by surrounding cells.

For the heterogeneous strains RCC1216 and CCMP371, AFLR correlation was clearly superior to the FLR correlation. However, the correlation could not be improved by using AFLR in the case of RCC1217, where the FLR correlation worked marginally better. In this case, the culture broth was very homogeneous over the entire cultivation, which made the weighing of heterogeneity rather unnecessary. It is therefore recommended to use the FLR correlation for RCC1217 and probably other non-calcifying strains. The AFLR/FLR correlation was shown to be a reliable method for the quantification of chlorophyll by single cell autofluorescence data. Nonetheless, it must be considered that AFLR/FLR is in fact a mathematical model, which creates links between measured information and biological properties. In any case, the presented method enables for the assessment of chlorophyll *a* content and growth with limited equipment. This may help to quickly evaluate the culture state without the need of a photometer or HPLC system.

### Acknowledgements

### References

1. Borowitzka MA (2013) High-value products from microalgae-their development and commercialisation. J Appl Phycol 25: 743-756.

2. Marques AE, Miranda JR, Batista AP, Gouveia L (2013) Microalgae biotechnological applications: Nutrition, health and environment. In: Johansen MN (eds) Microalgae: Biotechnology, Microbiology and Energy, Nova Science Publishers, Inc. Pp. 1-60.

3. Brownlee C, Taylor AR (2001) Algal Calcification and Silification, eLS, John Wiley & Sons, Ltd., USA.

4. Korbekandi HSI (2013) Biological Synthesis of Nanoparticles Using Algae. In: Rai M, Posten C (eds.), Green Biosynthesis of Nanoparticles - Mechanics and Applications, CABI.

5. Jena J, Pradhan N, Nayak RR, Dash BP, Sukla LB, et al. (2014) Microalga *Scenedesmus* sp.: A potential low-cost green machine for silver nanoparticle synthesis. J Microbiol Biotechnol 24: 522-533.

6. Hariskos I, Chairopoulou MA, Posten C, Teipel U, Vucak M (2015) Produktgestaltung in der Partikeltechnologie Band 7 - Produktion und Charakterisierung von biogenen, mikrostrukturierten Calcitpartikeln, Fraunhofer ICT 2015.

7. Krumov N, Posten C (2014) Nanostructured particles from coccolithophores - an undiscovered resource for applications. In: Wei G (eds) Green biosynthesis of nanoparticles: mechanisms and applications. CABI. Pp. 192.

8. Paasche EA (2001) A review of the coccolithophorid *Emiliania huxleyi* (Prymnesiophyceae), with particular reference to growth, coccolith formation, and calcification-photosynthesis interactions. Phycologia 40: 503-529.

9. Balch WM, Holligan PM, Kilpatrick, KA (1992) Calcification, photosynthesis and growth of the bloom-forming coccolithophore, *Emiliania huxleyi*. Cont Shelf Res 12: 1353-1374.

10. Feng Y, Warner ME, Zhang Y, Sun J, et al. (2008) Interactive effects of increased $pCO_2$, temperature and irradiance on the marine coccolithophore *Emiliania huxleyi* (Prymnesiophyceae). Eur J Phycol 43: 87-98.

11. Loebl M, Cockshutt AM, Campbell DA, Finkel ZV (2010) Physiological basis for high resistance to photoinhibition under nitrogen depletion in *Emiliania huxleyi*. Limnol Oceanogr 55: 2150-2160.

12. Ritchie RJ (2006) Consistent sets of spectrophotometric chlorophyll equations for acetone, methanol and ethanol solvents. Photosynth Res 89: 27-41.

13. Veldhuis MJW, Kraay GW (2000) Application of flow cytometry in marine phytoplankton research: Current applications and future perspectives. Sci Mar 64: 121-134.

14. Olson RJ, Zettler ER, Chisholm SW, Dusenberry JA (1991) Advances in Oceanography through Flow Cytometry. Particle Analysis in Oceanography, NATO ASI Series 27: 351-399.

15. Rutten TP, Sandee B, Hofman AR (2005) Phytoplankton monitoring by high performance flow cytometry: a successful approach? Cytometry A 64: 16-26.

16. Krause GH, Weis E (1991) Chlorophyll Fluorescence and Photosynthesis: The Basics. Annu Rev Plant Physiol Plant Mol Biol 42: 313-349.

17. Papageorgiou GC, Tsimilli-Michael M, Stamatakis K (2007) The fast and slow kinetics of chlorophyll *a* fluorescence induction in plants, algae and cyanobacteria: a viewpoint. Photosynth Res 94: 275-290.

18. Boussiba S, Bing W, Yuan JP, Zarka A, Chen F (1999) Changes in pigments profile in the green alga *Haematococcus pluvialis* exposed to environmental stresses. Biotechnol Lett 21: 601-604.

19. Danesi EDG, Rangel-Yagui CO, Carvalho JCM, Sato S (2004) Effect of reducing the light intensity on the growth and production of chlorophyll by *Spirulina platensis*. Biomass Bioenergy 26: 329-335.

20. Berges JA, Franklin DJ, Harrison PJ (2001) Evolution of an artificial seawater medium: Improvements in enriched seawater, artificial water over the last two decades. J Phycol 37: 1138-1145.

21. Baker NR (2008) Chlorophyll fluorescence: a probe of photosynthesis in vivo. Annu Rev Plant Biol 59: 89-113.

22. Olson RJ, Zettler ER, Anderson OK (1989) Discrimination of eukaryotic phytoplankton cell types from light scatter and autofluorescence properties measured by flow cytometry. Cytometry 10: 636-643.

23. Qin H, Li S, Li D (2012) An improved method for determining phytoplankton chlorophyll *a* concentration without filtration. Hydrobiologia 707: 81-95.

24. Limpert E, Stahel WA, Abbt M (2001) Log-normal distributions across the sciences: Keys and clues. BioScience 51: 341-352.

25. Salter C (2000) Error Analysis Using the Variance-Covariance Matrix. J Chem Educ 77: 1239.

26. McKew BA, Davey P, Finch SJ, Hopkins J, Lefebvre SC, et al. (2013) The trade-off between the light-harvesting and photoprotective functions of fucoxanthin-chlorophyll proteins dominates light acclimation in *Emiliania huxleyi* (clone CCMP 1516). New Phytol 200: 74-85.

27. Nanninga HJ, Tyrrell T (1996) Importance of light for the formation of algal blooms by *Emiliania huxleyi*. Mar Ecol Prog Ser 136: 195-203.

28. Paasche E (1999) Reduced coccolith calcite production under light-limited growth: a comparative study of three clones of *Emiliania huxleyi* (Prymnesiophyceae). Phycologia 38: 508-516.

29. MacIntyre HL, Kana TM, Anning T, Geider RJ (2002) Photoacclimation of photosynthesis irradiance response curves and photosynthetic pigments in microalgae and cyanobacteria. J Phycol 38: 17-38.

30. Rokitta SD, de Nooijer LJ, Trimborn S, de Vargas C, Rost B, et al. (2011) Transcriptome analyses reveal differential gene expression patterns between the life-cycle stages of *Emiliania huxleyi* (haptophyta) and reflect specialization to different ecological niches. J Phycol 47: 829-838.

31. Richier S, Kerros ME, Vargas C, Haramaty L, Falkowski PG, et al. (2009) Light-dependent transcriptional regulation of genes of biogeochemical interest in the diploid and haploid life cycle stages of *Emiliania huxleyi*. Appl Environ Microbiol 75: 3366-3369.

32. Posten C, Rosello-Sastre R (2000) Microalgae Reactors. Ullmann's Encyclopedia of Industrial Chemistry, Wiley-VCH Verlag GmbH & Co. KGaA.

33. Xu C, Auger J, Govindjee (1990) Chlorophyll *a* fluorescence measurements of isolated spinach thylakoids obtained by using single-laser-based flow cytometry. Cytometry 11: 349-358.

34. Neale PJ, Cullen JJ, Yentsch CM (1989) Bio-optical inferences from chlorophyll *a* fluorescence: What kind of fluorescence is measured in flow cytometry? Limnol Oceanogr 38: 1739-1748.

35. Sosik HM, Chrisholm SW, Olson RJ (1989) Chlorophyll fluorescence from single Cells: Interpretation of Cytometric signals. Limnol Oceanogr 34: 1749-1761.

36. Borman AH, de Jong EW, Huizinga M, Kok DJ, Westbroek P, et al. (1982) The role in $CaCO_3$ crystallization of an acid $Ca^{2+}$-binding polysaccharide associated with coccoliths of *Emiliania huxleyi*. Eur J Biochem 129: 179-183.